

XMM-NEWTON SPECTROSCOPY OF THE ACCRETION-DRIVEN MILLISECOND X-RAY PULSAR XTE J1751-305 IN OUTBURST

J. M. MILLER^{1,2,3}, R. WIJNANDS^{1,4,5}, M. MÉNDEZ⁶, E. KENDZIORRA⁷, A. TIENGO⁸, M. VAN DER KLIS⁸, D. CHAKRABARTY¹,
B. M. GAENSLER², AND W. H. G. LEWIN¹

Subject headings: binaries:close – pulsars: general – pulsars: individual: XTE J1751–305 – stars: neutron –
x-rays: binaries – white dwarfs

Draft version December 3, 2018

ABSTRACT

We present an analysis of the first high-resolution spectra measured from an accretion-driven millisecond X-ray pulsar in outburst. We observed XTE J1751–305 with *XMM-Newton* on 2002 April 7 for approximately 35 ks. Using a simple absorbed blackbody plus power-law model, we measure an unabsorbed flux of $6.6 \pm 0.1 \times 10^{-10}$ erg cm⁻² s⁻¹ (0.5–10.0 keV). A hard power-law component ($\Gamma = 1.44 \pm 0.01$) contributes 83% of the unabsorbed flux in the 0.5–10.0 keV band, but a blackbody component ($kT = 1.05 \pm 0.01$ keV) is required. We find no clear evidence for narrow or broad emission or absorption lines in the time-averaged spectra, and the sensitivity of this observation has allowed us to set constraining upper-limits on the strength of important features. The lack of line features is at odds with spectra measured from some other X-ray binaries which share some similarities with XTE J1751–305. We discuss the implications of these findings on the accretion flow geometry in XTE J1751–305.

1. INTRODUCTION

Millisecond radio pulsars are thought to be created in neutron star low-mass X-ray binaries (LMXBs). In those LMXBs, accreting matter may spin-up the neutron star (see, e.g., Bhattacharya & van den Heuvel 1991). Therefore, it is expected that millisecond pulsars should also be found in LMXBs during the accretion phase of the binary as X-ray pulsars. Although evidence for rapidly spinning neutron stars in LMXBs was inferred from the burst oscillations which were seen during type-I X-ray bursts in several systems (see Strohmayer 2001 for a review), the detection of millisecond pulsations in persistent emission remained elusive for many years. In 1998, the first such system was discovered (SAX J1808.4–3658, which has a spin frequency of 401 Hz; Wijnands & van der Klis 1998a). This source was extensively studied due to its obvious importance for binary evolution scenarios and accretion flow geometries and dynamics (see, e.g., Wijnands & van der Klis 1998b and references therein).

In the spring of 2002, Markwardt & Swank (2002a) reported the discovery of the second accretion-driven millisecond pulsar XTE J1751–305 (435 Hz) in the *Rossi X-ray Timing Explorer* (*RXTE*) bulge scan observation program. About one month after the discovery of this system, XTE J0929–314 was discovered (185 Hz; Remillard, Swank, & Strohmayer 2002.). The neutron stars in both systems are in orbit around a companion star, with an orbital period of ~ 42 minutes (Markwardt & Swank 2002b; Galloway et al. 2002). These systems are very tight binaries and the inferred mass of their companion stars is

very low ($\sim 0.01 M_{\odot}$).

After the discovery of XTE J1751–305, we submitted a target-of-opportunity request to *XMM-Newton* for the purpose of studying this source with high-resolution spectroscopy. The X-ray spectrum of the first system — SAX J1808.4–3658 — could only be studied during outburst using *RXTE* and with the Wide Field Cameras aboard *BeppoSAX*, which have only moderate spectral resolution. In this *Letter*, we present an analysis of the time-averaged EPIC-pn and Reflection Grating Spectrometer (RGS) data. The spectra obtained represent the first CCD- and gratings-resolution measurements from a millisecond X-ray pulsar in outburst.

2. OBSERVATION AND DATA REDUCTION

XMM-Newton observed XTE J1751–305 beginning on 2002 April 07.5 (UT). The EPIC-pn camera was operated in “timing” mode to prevent photon pile-up effects and to allow pulse-phase-resolved spectroscopy. The RGS was operated in the standard “spectroscopy” mode. The “thin” optical blocking filter was selected for the EPIC cameras. The EPIC-MOS cameras were not operated in modes optimized for a source of this intensity, and we do not consider the MOS spectra here.

The EPIC-pn and RGS data were reduced using SAS version 5.3. We applied the standard reduction procedure “epproc” to produce a calibrated pn event list. In “timing” mode, the spatial information is compressed into one dimension. We extracted source data in a rectangle (with a width of 37”) along the length of the CCD, and background data from adjacent regions; only

¹Center for Space Research and Department of Physics, Massachusetts Institute of Technology, Cambridge, MA 02139–4307

²Harvard-Smithsonian Center for Astrophysics, 60 Garden Street, Cambridge, MA 02138, jmmiller@head-cfa.harvard.edu

³National Science Foundation Astronomy and Astrophysics Fellow

⁴School of Physics and Astronomy, University of St. Andrews, St Andrews KY16 9SS, UK

⁵Chandra Fellow while at MIT

⁶SRON, National Institute for Space Research, Sorbonnelaan 2, NL-3584 CA, Utrecht, NL

⁷Institut für Astronomie und Astrophysik, Abt. Astronomie, Universität Tübingen, Sand 1, D-72076, Tübingen, DE

⁸Astronomical Institute “Anton Pannekoek”, University of Amsterdam, Kruislaan 403, NL-1098 SJ Amsterdam, NL

“single” and “double” events were selected. The net pn exposure was 33.7 ks. Using LHEASOFT version 5.1, the tool “grppha” was used to rebin the spectrum to require a minimum of 20 counts per bin. We used the trial “timing” mode redistribution and ancillary response functions developed by the EPIC-pn calibration team. We applied the standard reduction procedure “rgsproc” to produce calibrated RGS event lists, first-order spectra, and response functions. Periods of high instrumental background were excluded, giving a net RGS exposure of 34.2 ks. The RGS spectra were grouped to require at least 20 counts per bin.

3. ANALYSIS AND RESULTS

Preliminary spectroscopic results from this *XMM-Newton* observation were reported in Miller et al. 2002a and Miller et al. 2002b. The accurate position of XTE J1751–305 was reported by Ehle et al. (2002), also based on analysis of this observation (R.A. = $17^{\text{h}}51^{\text{m}}13.5^{\text{s}}$, Decl. = $-30^{\circ}37'22''$, equinox 2000.0).

The internal calibration accuracy of the EPIC cameras is better than 5% for on-axis sources (Kirsch 2002). We find deviations up to 0.6 keV which are not removed by spectral modeling, and therefore restrict our analysis of the pn spectrum to the 0.6–10.0 keV band. The average count rate ($79.36 \text{ counts s}^{-1}$) is well below that at which photon pile-up occurs in timing mode ($1500 \text{ counts s}^{-1}$). Tests of the effective area calibration of the RGS reveal accuracies of 5% in the $7\text{--}36\text{\AA}$ ($0.35\text{--}1.77 \text{ keV}$) range and 10% at wavelengths shorter than 7\AA (energies above 1.77 keV ; den Herder 2002). Although our best-fit model for the EPIC-pn spectrum (see below) provides an adequate fit to the RGS spectrum ($\chi^2/\nu = 1.314, \nu = 1463$), broad deviations are apparent at energies above 1.8 keV. We therefore rely on the EPIC-pn spectrum to characterize the continuum emission, and search the RGS band in contiguous 3\AA slices for narrow features.

The EPIC-pn and RGS spectra were analyzed using XSPEC version 11.1. All errors quoted in this paper are 90% confidence errors. Note that systematic errors are not added to the spectra to account for flux calibration uncertainties.

3.1. The EPIC-pn Spectrum

We first considered a model consisting of blackbody and power-law components, modified by neutral absorption in the ISM (using the “phabs” model in XSPEC). We measure a best-fit equivalent hydrogen column density of $N_H = (9.8 \pm 0.1) \times 10^{21} \text{ atoms cm}^{-2}$. The blackbody temperature obtained is moderate: $kT = 1.05 \pm 0.01 \text{ keV}$. For spherical symmetry, this translates into a blackbody radius of $R = f^2 \times 3.01_{-0.06}^{+0.09} (d/10 \text{ kpc}) \text{ km}$, where the spectral hardening factor f is the ratio of the color temperature and the effective temperature, and d is the distance to the source. The measured power-law index is $\Gamma = 1.44 \pm 0.01$; the normalization is $(6.4 \pm 0.1) \times 10^{-2} \text{ (photons keV}^{-1} \text{ cm}^{-2} \text{ s}^{-1} \text{ at 1 keV)}$. This model produces an adequate fit to the data: $\chi^2/\nu = 1.107$ (where ν is the number of degrees of freedom; $\nu = 1884$ for this model; see Figure 1). We note that a simple power-law model returns a very poor fit ($\chi^2/\nu > 4, \nu = 1886$); the soft blackbody component is strongly required by the data.

With this simple but standard model, we obtain an unabsorbed 0.5–10.0 keV flux of $(6.6 \pm 0.1) \times 10^{-10} \text{ erg cm}^2 \text{ s}^{-1}$, or $(0.170 \pm 0.004) \text{ photons cm}^{-2} \text{ s}^{-1}$. The hard power-law component contributes 83% of the unabsorbed flux

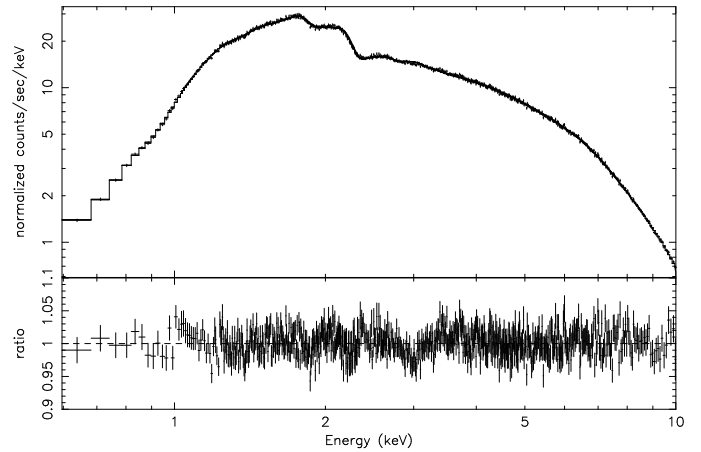


FIG. 1.— The EPIC-pn spectrum of XTE J1751–305, fit with a model consisting of blackbody and power-law components modified by photoelectric absorption (see Section 3 for details). The spectrum and data/model ratio shown above are rebinned for visual clarity.

in the 0.5–10.0 keV band (an extrapolation from the 0.6–10.0 keV band as the 0.5–10.0 keV range is more conventional).

Motivated by evidence for a Comptonizing volume in SAX J1808.4–3658 (Gierlinski, Done, & Barret 2002), we also fit the EPIC-pn spectrum with the “compTT” Comptonization model (Titarchuk 1994), which attempts to account for the Compton-upscattering of cool photons in a hot corona self-consistently. This model does not provide an acceptable fit by itself ($\chi^2/\nu = 2\text{--}4, \nu = 1884$). We find a degeneracy between a cool corona ($kT \sim 3 \text{ keV}$) with high optical depth ($\tau \sim 8$), and a hot corona ($kT \sim 40 \text{ keV}$) with lower optical depth ($\tau \sim 1$), each up-scattering a seed photon distribution peaking between $kT = 0.5\text{--}0.6 \text{ keV}$. Finally, we tried fitting a blackbody component in addition to compTT. This model might correspond to a scenario in which the blackbody emission region is only partially covered by the corona. This model also yielded a poor fit ($\chi^2/\nu \sim 2$).

The strength, ionization state, and profile of Fe $K\alpha$ emission lines — if produced through irradiation of the accretion disk — can reveal a great deal about the accretion geometry of low-mass X-ray binaries. Asai et al. (2000) report the possible detection of an Fe $K\alpha$ line in 4U 1820–30 ($P_{\text{orb}} = 11.4$ minutes; Stella, White, & Priedhorsky 1987). The line was found to be ionized ($E = 6.6 \pm 0.1 \text{ keV}$), broad ($\text{FWHM} = 0.7_{-0.5}^{+0.2} \text{ keV}$), and weak ($W_{K\alpha} = 33_{-11}^{+12} \text{ eV}$). Assuming a line of equivalent FWHM in the 6.40–6.97 keV range (Fe I — Fe XXVI), we measure a 95% confidence upper-limit of just 6 eV in the EPIC-pn spectrum of XTE J1751–305. Using a Gaussian with zero width to model a line narrower than the EPIC-pn resolution, the 95% confidence upper limit on the equivalent width of any such narrow Fe $K\alpha$ lines is less than 4 eV (6.40–6.97 keV).

3.2. Pulse-Phase-Resolved Spectroscopy: First Results

We applied the SAS task “barycen”, and using the binary system parameters reported by Markwardt et al. (2002) we produced spectra from the “high” and “low” parts of the pulse. We find that the model applied to the time-averaged spectrum is an acceptable description of these spectra (no convincing narrow or broad emission or absorption features are found). Interestingly, the slope of the power-law component is consistent in the two spectra but the normalization changes, and the blackbody component changes in temperature but not in normalization.

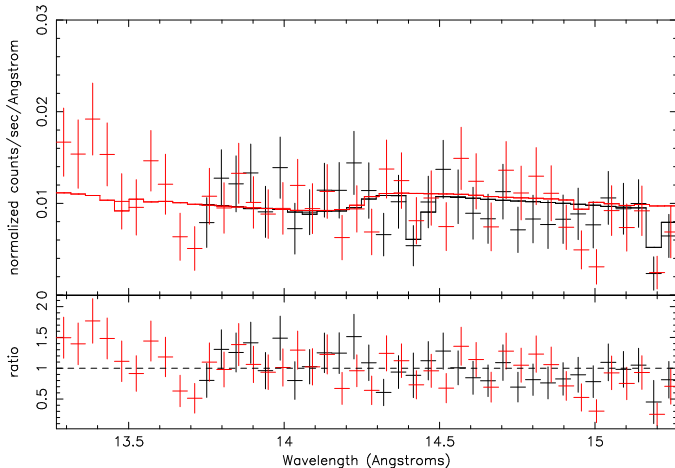


FIG. 2.— The RGS spectra of XTE J1751–305 (RGS-1 in black, RGS-2 in red; both are rebinned for clarity and narrow features are instrumental) fit locally in the region of the Ne K edge (14.25\AA) with a simple power-law plus edge model. The edge depth was fixed at the solar value but the power-law index and normalization were allowed to vary; a trend in the data/model ratio is clearly visible. Fits made with a variable edge depth suggest Ne is likely under-abundant (see text).

Similar behavior was discovered in pulse-phase-resolved spectra of SAX J1808.4–3658 (Gierlinski, Done, & Barret 2002).

We note that a possible feature at approximately 2.9 keV appears to vary in width, intensity, and centroid energy in the “high” and “low” spectra; however, the error limits on the line parameters overlap. This feature is also visible in the time-averaged spectrum (see Figure 1). As there are no astrophysically abundant elements with transitions near this energy, it is tempting to associate this feature with a red-shifted absorption line from the neutron star surface (given the temperature of the blackbody, perhaps Fe XXV or Fe XXVI). Although an F-test finds that the addition of a Gaussian to model this feature is significant at the 7σ level of confidence in the “low” part of the pulse (3σ in the “high” part), a similar feature is apparent when the EPIC-pn spectrum of the Galactic black hole candidate XTE J1650–500 (Miller et al. 2002c) is fit using the same response matrix. It is likely that this feature is due to a defect in the timing-mode response matrix.

3.3. The RGS Spectra

We analyzed the RGS spectra in contiguous 3\AA slices for narrow emission or absorption lines. In each 3\AA slice, a simple power-law plus ISM edge(s) model was fit to the data. We find no convincing evidence for narrow absorption features in this band (0.3–2.5 keV, or 5–40 \AA). At energies below ~ 0.6 keV (wavelengths longer than $\sim 21\text{\AA}$) the sensitivity is low due to the relatively high column density along the line of sight to XTE J1751–305.

Recently, evidence for enhanced Ne abundances has been found in compact binaries (Schulz et al. 2001; Juett, Psaltis, & Chakrabarty 2001). We fit the RGS spectra around the position of the Ne K edge (14.25\AA) with a power-law model between 13.25\AA and 15.25\AA (see Figure 2). The power-law index and normalization were both allowed to vary in this fit. Using the cross-sections of Verner et al. (1993) and solar abundances relative to H as per Morrison & McCammon (1983), we find that Ne may be *under*-abundant in XTE J1751–305:

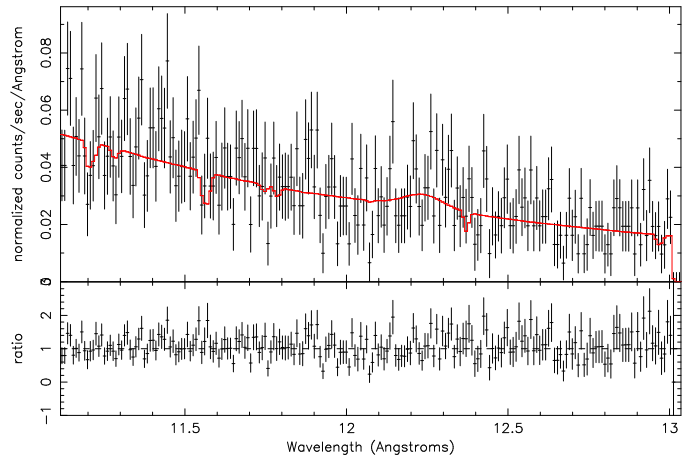


FIG. 3.— The RGS-2 spectrum of XTE J1751–305 in the region of the Ne X Ly- α line at 12.13\AA , fit with a simple power-law plus Gaussian model. Our best fit model does not require an emission line within $12.13 \pm 0.1\text{\AA}$, assuming a FWHM equivalent to the prominent Ne X Ly- α emission line seen in the 42-minute X-ray pulsar 4U 1626–67 (Schulz et al. 2001). Narrow features are instrumental.

the 95% confidence upper-limit is that the abundance of Ne is only 77% of the solar value. A solar Ne abundance does not allow for an optimal characterization of the local spectrum (see Figure 2).

The binary X-ray pulsar 4U 1626–67 also has a 42-minute orbital period. Moreover, the distance to this system may be close to 8 kpc (Chakrabarty 1998); we anticipate a Galactic center location for XTE J1751–305 and therefore a similar distance. A *Chandra*/HETGS spectrum of 4U 1626–67 reveals broadened emission lines and Doppler-shifted line pairs (Schulz et al. 2001). The Ne Ly- α line (12.13\AA) is particularly strong (a flux of $8.15 \pm 0.93 \times 10^{-5}$ photons $\text{cm}^{-2} \text{s}^{-1}$ is measured; FWHM = $2860 \pm 330 \text{ km s}^{-1}$). We report the 95% confidence upper-limits on emission lines from helium-like and hydrogenic Ne, Mg, and Si in Table 1 (upper limits on O emission lines are not constraining due to poor statistics at low energies).

4. DISCUSSION

We have analyzed the first CCD- and grating-resolution X-ray spectra of a millisecond X-ray pulsar in outburst. We find no convincing evidence for broad or narrow emission or absorption features in the the EPIC-pn and RGS spectra (see Figure 1 and Table 1). With our simple blackbody plus power-law model for the EPIC-pn spectrum, we find that the power-law component comprises 83% of the unabsorbed flux in the 0.5–10.0 keV band. The power-law component is hard: $\Gamma = 1.44 \pm 0.01$, but within a range typical for X-ray pulsars (e.g., $\Gamma = 1.0$ –1.5; White, Swank, & Holt 1983). The EPIC-pn spectrum requires a blackbody with $kT = 1.05 \pm 0.01$ keV and an implied emitting radius of $R = f^2 \times 3.01^{+0.09}_{-0.06}$ ($d/10\text{kpc}$) km. It is fair to say that our knowledge of the spectral hardening factor f is rather poor (for a discussion, see Lewin, van Paradijs, & Taam 1993). If f is less than 1.3, it would indicate that only part of the neutron star surface (a “hot spot”) is involved.

Markwardt et al. (2002) fit a simple absorbed power-law model to the *RXTE* spectrum of XTE J1751–305, and measure a softer power-law index ($1.7 < \Gamma < 1.9$). The effective lower sensitivity bound of the *RXTE* Proportional Counter Array (PCA) is 3 keV; fitting the 3–10 keV EPIC-pn spectrum with only a power-law, we find $\Gamma = 1.72 \pm 0.01$ for $N_H =$

$(9.8 \pm 0.1) \times 10^{21}$ atoms cm^{-2} and $\Gamma = 1.90 \pm 0.02$ allowing N_H to float (in this case, $N_H = [2.5 \pm 0.1] \times 10^{22}$ atoms cm^{-2}). Thus, the discrepant indices are easily explained in terms of different instrumental ranges.

In modeling simultaneous *Chandra*/LETGS and *RXTE* spectra of XTE J0929–314, Juett, Galloway, & Chakrabarty (2002) measure similarly discrepant power-law indices. They suggest an astrophysical origin for the discrepancy in XTE J0929–314 and XTE J1751–305 in the form of a power-law with a break or a roll-over in the 1.4–4.4 keV range. A model consisting of blackbody and broken power-law components ($E_{\text{break}} = 3.7 \pm 0.1$ keV, $\Gamma_{E < 3.7} = 1.34 \pm 0.03$, $\Gamma_{E > 3.7} = 1.60 \pm 0.04$) provides an improved fit to the spectrum of XTE J1751–305 ($\chi^2/\nu = 1.090$, $\nu = 1882$). Although these results suggest that an astrophysical origin for the apparent spectral evolution is possible, a number of concerns remain. Given that: (1) the effective area (flux) calibration of the EPIC-pn has 5% uncertainties (Kirsch 2002), (2) the LETGS (plus ACIS-S array) flux calibration has 10% uncertainties above 1 keV (H. Marshall, priv. comm.), (3) that *RXTE* PCA and High Energy X-Ray Timing Experiment (HEXTE) observations of the “Crab” nebula (taken to be a pure power-law for calibration) differ in power-law index by $\delta(\Gamma) \simeq 0.1$ (see, e.g., Wilms et al. 1999), and (4) that Markwardt et al. (2002) did not fit a blackbody component to the *RXTE* spectra of XTE J1751–305, we do not consider an astrophysical origin for the discrepant indices to be required by the present data.

The upper limits on the strength of narrow (consistent with instrument resolution; FWHM ~ 0.1 keV) and broad (FWHM = 0.7 keV) Fe $K\alpha$ emission lines are 4 eV and 6 eV, respectively (95% confidence). This stands in contrast the detection of a weak Fe $K\alpha$ line in outburst spectra of the 401 Hz millisecond X-ray pulsar SAX J1808.4–3658 obtained with *RXTE* (Heindl & Smith 1998; Gierlinski, Done, & Barret 2002). It is possible that a strong, hot corona (or the magnetosphere, if the coranae in these LMXBs is small or disrupted) which produces to the power-law component may ionize the disk in XTE J1751–305 to a degree which prevents Fe $K\alpha$ emission.

The absence of H-like and He-like resonance emission lines like those observed in 4U 1626–67 (Schulz et al. 2001) in the

spectrum of XTE J1751–305 is also consistent with a highly ionized disk in this source. Secondly, the absence of such lines may be due to differences in the accretion flow geometry due to the neutron star magnetic field. Whereas the magnetic field in XTE J1751–305 is likely to be similar to that in SAX J1808.6–3658 ($B = (2-6) \times 10^8$ G; Wijnands & van der Klis 1998a), the magnetic field in 4U 1626–67 is likely much higher ($B = 3 \times 10^{12}$ G, Orlandini et al. 1998). The stronger magnetic field in 4U 1626–67 may disrupt the inner disk, allowing cool material in the outer disk to be irradiated by a weaker corona. Emission lines have also been seen in neutron star systems which are viewed edge-on (so-called accretion disk coranae or “ADC” sources; see, e.g., Kallman et al. 2002); the absence of emission lines in XTE J1751–305 may also be partially due to a low system inclination (Markwardt et al. 2002 report no evidence of dips or eclipses).

Studies of some ultra-compact systems suggest a Ne-rich companion (for observational results, see: Schulz et al. 2001; Juett, Psaltis, & Chakrabarty 2001; for theoretical discussions see Yungelson, Nelemans, & van den Heuvel 2002; Bildsten 2002). Fits to the Ne photoelectric absorption edge in the RGS spectra of XTE J1751–305 constrain the abundance of Ne to be at most 77% of the solar value along this line of sight (95% confidence upper-limit; see Section 3.3). This may suggest that a Ne-rich companion is unlikely in the case of XTE J1751–305.

5. ACKNOWLEDGMENTS

We are grateful to the *XMM-Newton* Project Scientist Fred Jansen for granting time to observe this source. We thank Michael Nowak for useful discussions. J. M. M. is grateful for support from the NSF. R. W. was supported by NASA through Chandra fellowship grant PF9-10010, which is operated by the Smithsonian Astrophysical Observatory for NASA under contract NAS8-39073. W. H. G. L. gratefully acknowledges support from NASA. This work was supported in part by the Netherlands Organization for Scientific Research (NWO). This research has made use of the data and resources obtained through the HEASARC on-line service, provided by NASA-GSFC.

REFERENCES

- Arnaud, K. A., 1996, *Astronomical Data Analysis Software and Systems V*, eds. G. Jacoby and J. Barnes, p17, ASP Conf. Series vol. 101
- Asai, K., Dotani, T., Nagase, F., & Mitusda, K., 2000, *ApJS*, 131, 571
- Bhattacharya, D., & van en Heuvel, E. P. J., 1991, *Phys Rep.*, 203, 1
- Bildsten, L., 2002, *ApJ*, in press, astro-ph/0208164
- Bildsten, L., & Chakrabarty, D., 2002, *ApJ*, 557, 292
- Campana, S., et al., 2002, *ApJ*, in press, astro-ph/0206376
- Chakrabarty, D., 1998, *ApJ*, 492, 342
- Chakrabarty, D., & Morgan, E. H., 1998, *Nature*, 394, 346
- Ehle, M., et al., 2002, *IAU Circ.* 7872
- Galloway, T. R., Chakrabarty, D., Morgan, E., & Remillard, R., 2002, *ApJ*, in press, astro-ph/0206493
- Gierlinski, M., Done, C., & Barret, D., 2002, *MNRAS*, 331, 141
- Heindl, W. A., & Smith, D. A., 1998, *ApJ*, 560, 35L
- den Herder, J. W., 2002, RGS-SRON-RP-CAL-01/006, available at <http://xmm.vilspa.esa.es/ccf/documents/#general>
- Juett, A. M., Psaltis, D., & Chakrabarty, D., 2001, *ApJ*, 560, L59
- Juett, A. M., Galloway, D. K., & Chakrabarty, D., 2002, *ApJ*, submitted, astro-ph/0208543
- Kallman, T. R., Angelini, L., Boroson, B., & Cottam, J., 2002, *ApJ*, subm., astro-ph/0209010
- Kirsch, M., 2002, XMM-SOC-CAL-TN-0018, available at <http://xmm.vilspa.esa.es/ccf/documents/#general>
- Lewin, W. H. G., van Paradijs, J., & Taam R. E., 1993, *SSRv*, 62, 223
- Markwardt, C. B., & Swank, J. H., 2002a, *IAU Circ.* 7867
- Markwardt, C. B., & Swank, J. H., 2002a, *IAU Circ.* 7870
- Markwardt, C. B., Swank, J. H., Strohmayer, T. E., in ‘t Zand, J. J. M., & Marshall, F. E., 2002, *ApJ*, 575, L21
- Miller, J. M., et al., 2002a, *ATEL* 90
- Miller, J. M., et al., 2002b, *ATEL* 91
- Miller, J. M., et al., 2002c, *ApJ*, 570, L69
- Morrison, R., & McCammon, D., 1983, *ApJ*, 270, 119
- Orlandini, M., et al., 1998, *ApJ*, 500, 163L
- Remillard, R. A., Swank, J., & Strohmayer, T., 2002, *IAU Circ.* 7893
- Schulz, N. S., Chakrabarty, D., Marshall, H. L., Canizares, C. R., Lee, J. C., & Houck, J., 2001, *ApJ*, 563, 941
- Stella, L., White, N. E., & Priedhorsky, W., 1987, *ApJ*, 312, L17
- Strohmayer, T. E., 2001, *AdSpR*, 28, 511
- Titarchuk, L., 1994, *ApJ*, 434, 313
- Verner, D. A., Yakovlev, D. G., Band, I. M., & Trzhaskovskaya, M. B., 1993, *ADNDT*, 55, 233
- White, N. E., Swank, J. H., & Holt, S. S., 1983, *ApJ*, 270, 711
- Wilms, J., Nowak, M. A., Dove, J. B., Fender, R. P., & Di Matteo, T., 1999, *ApJ*, 522, 460
- Wijnands, R., & van der Klis, M., 1998a, *Nature*, 394, 344
- Wijnands, R., & van der Klis, M., 1998b, *ApJ*, 507, 63L
- Yungelson, L. R., Nelemans, G., & van den Heuvel, E. P. J., 2002, *A & A*, 388, 546

TABLE 1

Emission Line Upper-Limits

	Helium-like		Hydrogenic	
	Broad ^a (10 ⁻⁵ ph cm ⁻² s ⁻¹)	Narrow ^b (10 ⁻⁵ ph cm ⁻² s ⁻¹)	Broad ^a (10 ⁻⁵ ph cm ⁻² s ⁻¹)	Narrow ^b (10 ⁻⁵ ph cm ⁻² s ⁻¹)
Ne	1.6	1.4	0.9	0.5
Mg	1.4	1.3	11	8.8
Si	29	26	3.7	3.5

NOTE.—The 95% confidence upper limits on highly ionized resonance emission lines within 0.1Å of their expected rest-frame wavelengths in the RGS spectra of XTE J1751–305. ^a Assuming FWHM = 3000 km/s, similar to the Doppler-shifted pairs in 4U 1626–67 (Schulz et al. 2001). ^b The upper limits were calculated using Gaussians of zero width to model features narrower than the RGS resolution. Limits on the strength of O lines are not constraining due to poor statistics at low energies. These upper limits are similar to or below the fluxes measured from the lines detected in 4U 1626–67, indicating a constraining sensitivity was achieved in this *XMM-Newton* observation.